One Pot Bio-Synthesis of Palladium Nanoneedles and Its Bioavailability

Dnyaneshwar K. Kulal
University of Mumbai - Kalina Campus
Shubham V. Pansare
University of Mumbai - Kalina Campus
Amol A. Shedge
University of Mumbai - Kalina Campus
Shhyam Khairkkar
University of Mumbai - Kalina Campus
Shraddha Y. Chhatre
NCL: National Chemical Laboratory CSIR
Mohmad Vasim Sheikh
Ramnarain Ruia College, Mumbai
Vishwanath R. Patil
University of Mumbai - Kalina Campus
Amol V. Pansare (amol.pansare@empa.ch)
Empa Materials Science and Technology https://orcid.org/0000-0001-8133-1685

Research Article

Keywords: Palladium Nanoneedles, Aspergillus oryzae, Cancer Cell Lines, BSA, FRET theory, Antioxidant activity

Posted Date: June 28th, 2021

DOI: https://doi.org/10.21203/rs.3.rs-632642/v1

Abstract

Bioinorganic chemistry has achieved great importance by considering environmental and health issues. Here we present anticancer, antioxidant, good protein quencher single pot biosynthesized one dimensional palladium Nanoneedles (PdNNs) as a negative catalyst, where water plays a role of safer solvent. Needle-shaped one-dimensional PdNNs was synthesized using filamentous fungal stain of *Aspergillus oryzae* (biomass) was successively applied as a suppressant for the growth of human breast, colon and leukemia cancer Cell Lines. Quenching process of bovine serum albumin by PdNNs was spontaneous with hydrogen bonding and hydrophilic interaction. Interaction of protein and PdNNs showed binding constant in the range of 10^4 M^{-1} and one binding site. Forster's resonance energy transfer (FRET) theory applied to find out distance between the interaction of PdNNs and protein, where critical distance and energy transfer distance varies with change in concentrations of PdNNs 4.84 x 10^{-6} M to 9.69 x 10^{-7} M from 2.9 to 3.7 nm and 3.2 to 5.4 nm respectively. Radical scavenging method was applied to find out an antioxidant activity which of nanoneedles. Needle-shaped palladium nanoparticles and particle size found to be ≅ 3.0 nm using high-resolution transmission electron microscopes.

1. Introduction

Following all twelve green chemistry principles in chemical research is a difficult task. Which directly or indirectly correlated to human health, environment pollution, reduce or eliminate the use and generation of hazardous substances [1]. Therefore, a scientist tries to follow maximum green chemistry principles within the respective research area to avoid health and environmental hazards. Where green synthesized metal nanoparticles took great important due to unique chemical, optical, electronic, magnetic properties of metal nanoparticles [2], easy availability of bio-material and non-toxic reactant/product, while the whole process required less energy to synthesize such nanoparticle [3–5]. Recently our research group presented gold nanoparticles as an invisible barcode and its application [6, 7]. A literature survey indicates a different type of biomaterials were used for the nanoparticles synthesis as follows proteins [8], membranes [9], plant leaves [10], plant extracts [10] and whole cells of bacteria [11, 12], fungi [12], yeast [12] and algae [13]. When we consider properties of nanoparticles, the viability of large surface area for the reaction is a most important property, which categorizes them in the catalytic application. Depending on catalytic behavior in reactions catalyst categories in two types: the first is the positive catalyst, which increases the rate of reaction and second is the negative catalyst that suppressed the rate of reaction. Various metals and its composite was use for catalytic activities such as Co-N doped carbon [14], Ruthenium supported on ZIF-67 [15], cobalt [16, 17], Fe-doped CoP [1], and Pd [19–21]. While Pd nanoparticles used as catalyst in heck reaction [22] represents multistep synthesis root, requires massive energy, such as vacuum, pressure and toxic chemicals [3]. As well as palladium is well known for its catalytic activity as oxidative convertor of glycerol [23], as automotive catalyst [24], oil refining process [25], polyester manufacturing [26] and bacterial reduction of graphene oxide (GO) and Pd (II) salt supported *E. coli* utilized for production of H_2 and sodium formate [27]. Chemical synthesis of palladium nanoparticles was used chemicals such as NH_4OH [28], $NaBH_4$[29, 30], $SnCl_2$ [31] and bio-materials like

cupriavidus necator and cupriavidus metallidurans [32], *gardenia jasminoides* [33], bark extract of *cinnamom zeylanicum* [34], *plectonema boryanum* [2], *desulfovibrio desulfuricans* [35], *shewanella oneidensis* [36], *escherichiacoli* [37], *desulfovibrio fructosivorans* [38], *clostridium pasteurianum* [39], coffee [40] and tea [40] extract as a cost-effective method. Among that chemical synthesis method is complicated, using harsh conditions and chemicals will show side-effect on human health. Hence simple and non-toxic biosynthesis method for Pd nanoparticles synthesis is necessary for the catalytic application.

Here we synthesize palladium nanoparticles using fungal stain of *aspergillus oryzae* which is non-toxic in nature, as it was utilized in the food industry. China and East Asian Countries used *aspergillus oryzae* for making soy sauce and bean paste from fermented soybeans. It also used in the making of alcoholic beverages, such as *huagjiu*, *sake*, *makgeojli* and *shochu*. This indicates that *aspergillus oryzae* is shown rapid growth, non-toxic in nature, easily availability, safe to handle in the laboratory and commercially utilized for the fermentation process. Therefore, the fungal stain of *aspergillus oryzae* is selected for PdNNs synthesis.

This article presents quick, simple, one pot green synthetic method for synthesis of palladium nanoparticles (Scheme 1) using fungal stain of *aspergillus oryzae* in a safer solvent. Green synthesized PdNNs shows good anticancer activity [41–43] with human breast adenocarcinoma cell lines MCF-7, where it inhibits a growth of breast cancer cell lines. Interaction of PdNNs–BSA was studied at a various temperature to calculated kinetic parameters like entropy (ΔS°), enthalpy (ΔH°) and free energy (ΔG°) and also find out interaction distance between PdNNs–BSA using FRET theory. Good antioxidant activity of PdNNs was observed using DPPH radical scavenging method.

2. Experimental Section

2.1 Materials and Methods

All chemicals used in this work were of analytical reagent grade. A laboratory strain of lyophilized a*spergillus oryzae* obtained from National Collection Industrial Micro-organism (NCIM), Pune, India was used for sterilization. BSA was purchased from Sigma Aldrich, India. Glassware's were properly washed with double distilled water and autoclaved at 121°C for about 20 min. Palladium chloride ($PdCl_2$) was purchased from s. d. fine- chemical Limited.

2.2 Preparation of *Aspergillus oryzae* Stain

Aspergillus oryzae cultivated in solid media composed of sabouraud dextrose broth 30 g L^{-1} and agar 20 g L^{-1} was used for the growth of the fungal biomass, which was preserved by refrigerating at 4°C. The starter culture was prepared by loop full inoculation of the cultivated fungus in 100 mL liquid medium (without agar) which was followed by 48 hrs incubation at 25°C. The experimental culture was prepared using 250 mL of liquid medium inoculated with 5 mL of the starter culture then stored for 25 days at 25°C. The growth media was then centrifuged at 7500 rpm for 30 min for separation of biomass and

extract. The solid fungal biomass was used for sorption of metal from the environment by solid phase extraction method and extract utilized for the synthesis of PdNNs. The working solution was preserved at 4°C.

2.3 Synthesis of Palladium Nanoneedles

Pd(II) stock solution was prepared by dissolving an appropriate amount (177.3 mg/100mL) of $PdCl_2$in a protic solvent. From above stock solution, 10 mM palladium solution was prepared. 25 ml (10 mM) palladium solution was added in 965 mL of double distilled water followed by 10 ml reducing agent kept on the magnetic stirrer. The reaction mixture was stirred on 700 rpm at 55°C temperature for reduction of palladium ions to the nanoneedles, which was monitored by UV-Visible spectroscopy in the range of 200–800 nm on Lab UV 3000 plus double beam spectrophotometer. UV-Visible spectroscopy is a technique which gives an idea about change in color whereas in the case of nanoneedles it gives a probable idea about the reduction of metal ion to nanoneedles formation. The color of reaction mixture changes from light yellow to dark brown which indicates the reduction of $PdCl_2$ to PdNNs.

2.4 Separation of biosynthesized PdNNs from fungal stain

To separate PdNNs of approximately 2 to 25 nm in size from A*spergillus oryzae* fungal stain, Solution containing PdNNs was centrifuged at 11000 rpm for 30 min from larger clusters using research centrifuge made by REMI ISO 9001:2000 certified with a capacity of 17300 rpm. Centrifuged PdNNs were settled down to the bottom due to applied of centrifugal as well as gravitational force. The settled nanoneedles then re-suspended in a small amount of ethanol using ultra sonicator. Suspended nanoneedles were dried at room temperature for avoiding agglomeration of particles. The PdNNs powder was used for further study.

2.5 BSA binding experiments

All the experiments involving the interaction of the PdNNs with BSA were performed in phosphate buffer (0.1M) medium. A stock solution of BSA was prepared by dissolving an appropriate amount of BSA in a phosphate buffer medium and 1 hr. kept for stirring, which was then preserved in a refrigerator at 4°C in a dark atmosphere and used within 2 h. The absorption spectra of the BSA in the absence and presence of successive additions of the stock solution and the palladium complex were measured at 280 nm and changes in the BSA absorption were recorded after each addition. The strong fluorescence response of BSA provides a sensitive spectroscopic method to study the interaction with different molecules. The fluorescence emission spectra were recorded in the wavelength range of 250–500 nm by exciting the BSA at 278 nm, with the excitation and emission slit widths of 5 nm. Different concentrations of PdNNs (9.69 x 10^{-7} M to 4.84 x 10^{-6} M) were prepared by serial dilution of stock solution. All the solutions were sonicated for 5 min and kept for incubation for 20 min then allowed to equilibrate for 10 min after each addition. The fluorescence emission spectra were recorded at three different temperatures 293 K, 298 K, and 310 K (Fig. S1 to S3 respectively).

2.6 Determination of synchronous fluorescence spectra

In order to confirm the binding sites of PdNNs to BSA molecules, the synchronous fluorescence spectra of BSA solutions along with a gradual increase of PdNNs concentrations were collected in wavelength ranges from 245 nm to 400 nm for Δλ = 15 nm (Fig. S4) (for tyrosine residues) and from 290 nm to 400 nm for Δλ = 60 nm (Fig. S5) (for tryptophan residues) respectively. Excitation and emission slit width was set at 5.0 nm.

2.7 Effect of PdNNs on the conformation of BSA using CD

The spectra were recorded using JASCO, J-815 CD spectrometer and 1 cm path length quartz cell was used. The measurements were taken in the UV region at the wavelength range of 200–260 nm with band width of 5.0 nm for the concentration of plane BSA ($6.25X10^{-6}$ to $2.50X10^{-5}$M).

2.8 In vitro anticancer study

The human cancer cell lines MCF-7, Colo-205 and K562 were propagated in RPMI1640 medium made up of 10% fetal bovine serum, 2 mM L-glutamine at 37°C in 5% CO_2 atmosphere, 95 % air and 100 % relative humidity for 24 hrs. Sulforhodamine B dye (SRB) based in vitro cytotoxicity assay was performed to compare anti-tumor effects of PdNNs and standard drug Adriamycin (ADR) against MCF-7, COLO-205 and K562 cell line using method reported in the literature [43]. MCF-7, COLO-205 and K562 cell lines were maintained in RPMI1640 medium, 10% fetal bovine serum, 2 mM L-glutamine at 37°C in 5% CO_2 and 95% air atmosphere. Cells were inoculated into 96 well microtiter plates in 90 µl at plating densities 5×10^{-3} cells/ml. Every drug was tested in 4 times in 4 wells at similar conditions. After incubating the cells in a logarithmic phase with free ADR, different concentrations of PdNNs solution in different concentrations (1.0×10^{-7} M, 1.0×10^{-6} M, 1.0×10^{-5} M and 1.0×10^{-4} M) were prepared by serial dilution of stock solution, Sulforhodamine B dye 50 µl (0.4 % (w/v) in 1% acetic acid) was added to each well. After incubation for 4 hrs, the percentage of cell viability was determined at 540 nm and 690 nm relative to non-treated cells. To investigate the targeting ability of the MCF-7, Colo-205 and K562 cancer cells with the addition of PdNNs and ADR, plates were incubated at standard conditions for 48 hours and the assay was terminated by the addition of cold trichloroacetic acid (TCA). Cells were fixed *in situ* by the gentle addition of 50 µl of cold 30% (w/v) TCA (final concentration, 10% TCA) and incubated for 60 min at 4°C. The supernatant was discarded; the plates were washed five times with double distilled water and dried in air. SRB solution (50 µl) at 0.4% (w/v) prepared in 1 % acetic acid was added to each of the wells, and plates were incubated for 20 minutes at room temperature. After staining, the unbound dye was recovered and the residual dye was removed by washing five times with 1% acetic acid. The plates were air dried. The bound stain was subsequently eluted with 10 mM trizma base, and the absorbance was recorded on an Elisa plate reader at a wavelength of 540 nm with 690 nm using as a reference wavelength.

2.9 DPPH radical scavenging activity method

The hydrogen atom or electron donation ability of the PdNNs was measured from the bleaching of the purple colored methanol solution of 1,1-diphenyl-1-picrylhydrazyl (DPPH) [44]. Antioxidant activity of PdNNs was determined by DPPH (2, 2-diphenyl-1-picrylhydrazyl) assay. A Stock solution of DPPH free radical in ethanol (2.16 mg/50 ml) was prepared. 1 mL of various concentrations of the PdNNs (25, 50,

75, 100 and 125 µg/ml) in ethanol was compared with the same concentration of L-ascorbic acid (AA) was used as standards. Sample kept 30 min of incubation at room temperature in a dark atmosphere; the absorbance was measured against blank at 517 nm. Percent of inhibition (I%) of free radical production from DPPH by PdNNs and AA was calculated.

3. Result And Discussion

UV-Visible spectra of 0.5 mM palladium solution were reordered before and after synthesis of PdNNs compared with plane *aspergillus oryzae* extract. PdNNs was synthesized within 1 hrs after addition of *aspergillus oryzae* extract (Fig. 1a). The peak observed at 307 nm and 423 nm indicated the presence of Pd^{2+} in palladium chloride solution [45]. One hour of stirring at 65˚C with *aspergillus oryzae* extract, peak observed in palladium chloride solution at 307 nm was completely disappeared and a new absorption peak was observed at about 410 nm instead of 423 nm, which indicated the formation of PdNNs [46].

The X-ray diffraction data was applied to determine the orientation of the crystallographic planes of biosynthesized PdNNs. The reflection pattern of the PdNNs for the untreated sample in the angle of the 2θ range is delineated in Fig. 1b, which shows following patterns: peak1 (110), peak2 (200), and peak3 (220) reflections at 39.61, 46.11, and 67.43 respectively. Since *h*, *k* and *l* are always integers, we can obtain $h^2 + k^2 + l^2$ values by dividing the $\sin^2\theta$ values for the different XRD peaks with the minimum one in the pattern. The $h^2 + k^2 + l^2$ value sequence of the peak was 3, 4, 8 respectively which was in agreement with the sequence of the Face-centered cubic pattern. These observations conclude that PdNNs were in a Face-centered cubic lattice form [47]. Whereas the unit-cell parameters for patterns 3.9411 A^0 were calculated (using formulae presented in S1).

The morphology and size of the synthesized Nanoneedles were determined by TEM analysis. Typical TEM images obtained for PdNNs showed Nanoneedles of average particle size 3.0 nm width (Fig. 2) (calculated using ImageJ Software and respected value showed in **Table S1)**. The data was supported by EDAX analysis, where the peaks correspond to the binding energy at 2.83 keV confirmed presence of Pd in respected PdNNs sample (Fig. S6).

Interaction of PdNNs with BSA results in complex formation was studied by UV–visible, Fluorescence spectroscopy and Circular dichroism spectroscopy (CD). BSA made up of tryptophan, tyrosine and phenylalanine, which shows absorption peak at 280 nm in UV–visible spectroscopy (Fig. S7) [48]. When BSA forming a complex with PdNNs at different concentrations absorption of complex get increased was depicted in Fig. 3f.

Fluorescence spectroscopy was used to identify the quenching mechanism and the strength of the interaction between BSA with PdNNs. Whereas quenching usually shows two types of mechanisms (dynamic and static) depending on the way of interaction between BSA and quencher [49]. Interaction of BSA and PdNNs was recorded by fluorescence spectroscopy with an increasing amount of PdNNs. It indicates that the fluorescence intensity of BSA was inversely proportional to the increasing

concentration of PdNNs. In order to explore the effect of the interaction of BSA, with the various concentrations of PdNNs (9.69 x 10^{-7} M to 4.84 x 10^{-6} M), (Fig. 4a) the fluorescence quenching data at different temperatures were analyzed by using Stern-Volmer equation (**S2**) [46]. The value of quenching constant decreases with increasing temperature; this indicated that binding between PdNNs and BSA by complex formation resulted in successful quenching. The value of kq was calculated by considering the average lifetime of protein without the presence of quencher and its value was 10^{-8}s [50]. The maximum scattering collision quenching constant of various quenchers with the biopolymer is 2×10^{10} L mol^{-1} s^{-1} which was reported in the literature [51]. In the present work, the quenching constant k_q was in the order of 10^{13} L mol^{-1} s^{-1} which clearly indicated that the interaction between BSA and PdNNs was accured through a static quenching process [51]. Binding mechanism gives (**S3**) binding constant (K) between BSA and PdNNs was found in the range of 10^4 M^{-1} and number of binding sites (n) between BSA and PdNNs was approximately equal to 1 delineated in **Table S3**. Which suggested that PdNNs can easily be complex in protein as well as released in desired target areas and shows moderate affinity [52, 53].

Inorganic molecules interact with BSA by various forces namely hydrogen bonding, electrostatic interaction, van der waals interactions, hydrophilic, and hydrophobic interactions. Which was identifies using Van't Hoff equation (**S4**) by evaluating the value of the change in entropy ($\Delta S°$) and enthalpy ($\Delta H°$) for the binding reaction which further gives Gibbs free energy ($\Delta G°$) showed in **Table S4**. The negative value of free energy ($\Delta G°$) showed that the binding process was spontaneous. In the BSA and PdNNs interaction, the negative value of ΔS° (-274.832 $Jmol^{-1}K^{-1}$) indicates hydrophilic interaction. A negative value of ΔH° (-109.295 $KJmol^{-1}$) indicated the hydrogen bonding between BSA and PdNNs [54].

The fluorescence of BSA was observed due to the presence of Tyrosine residues and Tryptophan residues. Among this tryptophan is the most dominant fluorophore. Most of the metals were bind to one of the active bind sites of protein present in BSA. To find out the binding site synchronous method is used which gives conformational changes in protein molecules. When the difference (Δλ) between excitation wavelength and the emission wavelength was at 15 nm and 60 nm where quenching of the fluorescence intensity indicative of tyrosine and tryptophan residues respectively. The synchronous fluorescence spectra of BSA solutions were recorded in the presence of Nano-sized PdNNs with the increasing concentration by 10min ultra sonication and 20 min incubation treatments (**Fig. S6, S7**). The fluorescence intensities of tryptophan, as well as tyrosine, reduces consistently by addition of PdNNs but during the interaction, the emission wavelength of the tryptophan residues shows a blue shift with increasing concentration of PdNNs. Whereas tyrosine does not show any conformational change in emission wavelength by addition of PdNNs. It indicates that the interaction of PdNNs with protein affects the conformation of a tryptophan residue. The synchronous measurements confirmed the effective binding of PdNNs with BSA. Hence the strong interaction of these complexes with BSA suggests that the PdNNs may be suitable for anticancerous studies [55].

The CD spectra of BSA with and without PdNNs were measured and delineated in Fig. 3d, There were two negative peaks observed in the CD spectra region at around 208 and 222 nm, which are the

characteristics of α- the helical structure of the protein (BSA) [56]. Where MRE_{208} was the observed MRE value at 208 nm, 4000 was the MRE of the β-form and random coil conformation cross at 208 nm, whereas 33000 was the MRE value of α-helix at 208 nm. By using the equation (**S5**), the percentage of α -helix of BSA was calculated. The percentage of helicity of BSA was decreased with increasing concentration of PdNNs nanoparticles. The content of α-helix was decreased from 59.79 to 57.47% at 208 nm and 51.10 to 46.68% at 222 nm showed in **Table S5**. CD analysis confirmed that the binding of BSA with PdNNs alter the secondary structure of BSA.

According to Forster's resonance energy transfer (FRET) theory, donor fluorophore in its excited state transfers its energy to an acceptor molecule through the non-radiative dipole-dipole coupling, whereas the donor-acceptor distance at which energy transfer is 50% efficient is referred to as the critical distance (R_0). The efficiency of this energy transfer can be used to estimate the distance (r) between the PdNNs and fluorophore in the biomolecule [57, 58]. This energy transfer depends on the extent of overlap of the emission spectrum of the donor with the absorption spectrum of the acceptor [59]. The values of R_0 and r were calculated from equation (**S6**) for concentrations from 4.84 x 10^{-6} M to 9.69 x 10^{-7} M varies to 2.9 to 3.7 nm and 3.2 to 5.4 nm respectively tabulated in **Table S6**. The shortest donor-acceptor distance arises from FRET between a pair of donor and acceptor. The result showed that PdNNs were strong quencher and they were situated at close proximity to the BSA fluorophore.

The bio-synthesized PdNNs were screened in vitro for anticancer activity against Human Breast Cancer Cell Line MCF-7, COLO-205 and K562. First time we present needle shaped palladium nanoparticles was applied for anticancer study respective literature tabulated in **Table S7**. The results were expressed in the form of concentration that resulted in a 50% inhibition (IC50 values) whereas the well-known anticancer agents Adriamycin were used for positive controls. GI_{50} Growth inhibition of 50% was calculated in triplicate for different concentrations of PdNNs such as 10^{-7}, 10^{-6}, 10^{-5} and 10^{-4} M gives average values (**Table S8)** for cancer cell line MCF-7, COLO-205 and K562 shows in Fig. 5a-c indicated that green synthesized PdNNs showed positive activity against Human Breast Cancer Cell Line MCF-7, COLO-205 and K562.

The ability to trap free radicals is the main property of any antioxidant compound. Therefore, PdNNs has studied for the potential bio-synthesized antioxidant agent. Antioxidant activity was estimated by using the DPPH radical scavenging assay method, were AA consider as a standard antioxidizing agent with which PdNNs property was compared. The DPPH has a half fielded electron configuration so it has the ability to accept an electron or hydrogen free radical. Exactly antioxidant property means odd electron from DPPH forming a pair due to 'H' transfer from an antioxidant it results in decrease its absorbance [58]. PdNNs showed antioxidant activity. The higher radical scavenging activity against DPPH (Fig. 6) shows for the concentration of 125µg/ml as 53%.

4. Conclusion

In summary, the present investigation is based on a bio-synthesis of needle-shaped PdNNs using fungal biomass, economically favourable and simple. Needle-shaped one-dimensional palladium nanoparticles synthesis carried out in a single pot. BSA and PdNNs are spontaneous hydrogen binding process showed hydrophilic interaction revealed by emission studies. In quenching and binding process of PdNNs with BSA conclude that nanoneedles is a static binder and quencher for BSA. Forster radii and overlap integral values indicated the occurrence of an efficient FRET process between the albumins and the PdNNs. Conclusive antioxidant properties of bio-synthesized PdNNs showed anticancer activity against human cancer Cell Lines, which suggested its future demand in the field of bio inorganic medicine. Further study focus on reusability of palladium nanoparticles by synthesizing magnetic palladium nanoparticles.

Declarations

Author contributions

Amol Pansare and Vishwanath Patil designed the conceived the project and designed the experiments. All experiments were performed by Dnyaneshwar Kulal, Shubham Pansare, Amol Shedge and Shhyam Khairkkar. Charactrization data was analyzed by Dnyaneshwar Kulal, Shubham Pansare, Amol Shedge, Shhyam Khairkkar, Shraddha Chhatre and Mohmad Vasim Sheikh. All authors helped in the interpretation of the data and contributed to writing the manuscript.

Funding and acknowledgments

Dnyaneshwar K. Kulal acknowledge University of Mumbai, India, for funding. Amol V. Pansare acknowledges Composites Group, Mechanical Systems Engineering, Swiss Federal Laboratories for Materials Science and Technology-Empa, 8600 Dübendorf, Switzerland for funding.

Ethics Approval Not applicable.

Consent to Participate Not applicable.

Consent for Publication Not applicable.

Competing Interest The authors declare no competing interests.

References

1. Anastas, P. T., & Williamson, T. C. (1996). *Green Chemistry: Designing Chemistry for the Environment* (pp. 1–17). American Chemical Society
2. Lengke, M. F., Fleet, M. E., & Southam, G. (2007). *Langmuir*, 23, 8982–8987
3. Pugazhenthiran, N., Anandan, S., Kathiravan, G., Kannaian, N., Prakash, U., Crawford, S., & Ashokkumar, M. (2009). *J. Nanopart. Res*, 11, 1811–1815
4. Jia, L., Zhang, Q., & Li, Q. (2009). *andH. Song, Nanotechnology*, 20, 385601

5. Song, J. Y., Kwon, E. Y., & Kim, S. B., Bioprocess Biosyst. Eng. 33 (1)(2010). 159–164.
6. Tan, E. K. W., Shrestha, P. K., Pansare, A. V., Chakrabarti, S., Li, S., Chu, D. … Nagarkar, A. A. (2019). *Adv. Mater*, 1901802. doi.org/10.1002/adma.201901802
7. Pansare, A. V., Khairkar, S. R., Shedge, A. A., Chhatre, S. Y., Patiland, V. R., & Nagarkar, A. A. (2018). *Adv. Mater*, 30(33), 1801523. doi:10.1002/adma.201801523
8. Iwahoriandl, K., & Yamashita (2007). *J. Clust. Sci*, 18, 358–370
9. Konishi, Y., Tsukiyama, T., Tachimi, T., Saitoh, N., Nomura, T., & Nagamine, S. (2007). *Electrochim. Acta*, 53, 186–192
10. Song, J. Y., & Kim, B. S. (2009). *Biosyst. Eng*, 32, 79–84
11. Mandal, D., Bolander, M. E., & Mukhopadhyay, D. (2006). G. Sarkar andP. Mukherjee. *Appl. Microbiol. Biotechnol*, 69, 485–492
12. Gerickeand, M., & Pinches, A. (2006). *Hydrometallurgy*, 83, 132–140
13. Davisa, T. A., & Mucci, B. V. A. (2003). *Water Res*, 37, 4311–4330
14. Song, J., Ren, Y., Li, J., Huang, X., Cheng, F., Tang, Y., & Wang, H. (2018). *Carbon*, 138, 300–308
15. Tuan, D. D., Kun-Yi, A., & Lin (2018). *Chem. Eng*, 351, 48–55
16. Liu, H., Xu, S., Zhoua, G., Huang, G., Huang, S., & Xiong, K. (2018). *Chem. Eng*, 351, 65–73
17. Keane, T. P., Brodsky, C. N., andD, G., & Nocera (2019). *Organometallics*, 38(6), 1200–1203
18. Qin, X., Wang, Z., Han, J., Luo, Y., Xie, F., Cui, G. … Sun, X. ChemComm. 54 (55)(2018). 7693–7696.
19. Liu, J., Zhou, X., Rao, H., Xiao, F., Li, C. J., & Deng, G. J. (2011). *Chem. Eur. J*, 17, 7996–7999
20. Liu, S., Wang, H., Dai, X., & Shi, F. (2018). *Green Chem*, 20, 3457–3462
21. Liu, H., Jiang, T., Han, B., Liang, S., & Zhou, Y. (2009). *Science*, 326(5957), 1250–1252
22. Chung, D. S. C., Lee, J. S., Ryu, H., Park, J., Kim, H., Lee, J. H. … Lee, M. H. B. S. (2018). *Angew. Chem. Int. Ed*, 57(47), 15460–15464
23. Bambagioni, V., Bevilacqua, M., Bianchini, C., Filippi, J., Lavacchi, A., & Marchionni, A. (2010). F. Vizza andP. K. Shen, ChemSusChem. 3851–855.
24. Meel, V., Smekens, K., Behets, A., Kazandjian, M., Van, P., & Grieken, R. (2007). *Anal. Chem*, 79, 6383–6389
25. Damin, I. C., Vale, M. G. R., Silva, M. M., Welz, B., Lepri, F. G., Santos, W. N., & Ferreira, S. L. J Anal At Spectrom. 20(2005). 1332–1336.
26. Furst, M. R. L., Goff, R. L., Quinzler, D., & Mecking, S. (2012). C. H. Botting andD. *J. Cole-Hamilton, Green Chem*, 14, 472–477
27. Priestley, R. E., Mansfield, A., Bye, J., Deplanche, K., Jorge, A. B., Brett, D. … Sharma, S. (2015). *RSC Adv*, 5(102), 84093–84103
28. Atyaoui, M., Atyaoui, A., Khalifa, M., Elyagoubi, J., Dimassi, W., & Ezzaouia, H. (2016). *Superlattices Microstruct*, 92, 217–223
29. Bhardwaj, M., Sahi, S., Mahajan, H., Paul, S., & Clark, J. H. (2015). *J Mol Catal A Chem*, 408, 48–59

30. Feliciano-Ramos, I., Ortiz-Quiles, E. O., Cunci, L., Díaz-Cartagena, D. C., Resto, O., & Cabrera, C. R. (2016). *J SOLID STATE ELECTR*, 20, 1011–1017
31. Tan, D. C. L., Khezri, B., Amatyakul, W., Webster, D., Richard, D., & Sato, H. (2015). *RSC Adv*, 5(108), 88805–88808
32. Gauthier, D., Sobjerg, L. S., Jensen, K. M., Lindhardt, A. T., Bunge, M., Finster, K. … Skrydstrup, T. ChemSusChem. 3(2010). 1036–1039.
33. Akhtar, M. S., Panwar, J., & Yun, Y. S. (2013). *ACS SUSTAIN CHEM ENG*, 1(6), 591–602
34. Bankar, A., Joshi, B., Kumar, A. R., & Zinjarde, S. (2010). *Mater. Lett*, 64(18), 1951–1953
35. Mikheenko, I. P., Bennett, J. A., & Shannon, I. J. (2009).J. Wood andL. E. Macaskie, Adv. Mat. Res.71–73725–728.
36. Ogi, T., Honda, R., Tamaoki, K., Saitoh, N., & Konishi, Y. (2011). *Powder Technol*, 205, 143–148
37. Bunge, M., Sobjerg, L. S., Rotaru, A. E., Gauthier, D., Lindhardt, A. T., Hause, G. … Meyer, R. L. (2010). *Biotechnol. Bioeng*, 107, 206–215
38. Mikheenko, P., Rousset, M., Dementinand, S., & Macaskie, L. E. (2008). *Appl. Environ. Microbiol*, 74, 6144–6146
39. Chidambaram, D., Hennebel, T., Taghavi, S., Mast, J., Boon, N., Verstraete, W. … Fitts, J. P. (2010). *Environ. Sci. Technol*, 44(19), 7635–7640
40. Nadagouda, M. N., & Varma, R. S. (2008). *Green Chem*, 10, 859–862
41. Gurunathan, S., Kim, E., Han, J. W., Park, J. H., & Kim, J. H. (2015). *Molecules*, 20(12), 22476–22498
42. Kanchana, M., Savithaand, D., & Jeevitha, D. (2014). *World J. Pharm. Res*, 3(1), 765–784
43. Ghosh, S., Nitnavare, R., Dewle, A., Tomar, G. B., Chippalkatti, R., More, P. … Chopade, B. A. (2015). *Int J of nanomedicine*, 10, 7477–7490
44. Burits, M., & Bucar, F. (2000). *Phytother. Res*, 14, 323–328
45. Petla, R. K., Vivekanandhan, S., Misra, M., Mohanty, A. K., & Satyanarayana, N. (2012). *J Biomater Nanobiotechnol*, 3, 14–19
46. Tang, S., Vongehr, S., Zheng, Z., Ren, H., & Meng, X. Nanotechnology. 23(25)(2012). 255606/1-255606/11.
47. Lab1_2009 base,INDEXING DIFFRACTION PATTERNS FROM CUBIC MATERIALS
48. Li, D., Zhu, M., Xu, C., & Ji B., Eur. J. Med. Chem. 46(2)(2011). 588–599.
49. Callis, P. R. (2014). *J. Mol. Struct*, 1077, 14–21
50. Wei, Y. L., Li, Q., Dong, C., Shuang, S. M., Liu, D. S., & Huie, C. W. (2006). *Talanta*, 70, 377–382
51. Lakowicz, J. R., & Webber, G. (1973). *Biochemistry*, 12, 4161–4170
52. Pansare, A. V., Kulal, D. K., Shedge, A. A., & Patil, V. R. (2016). *Dalton Trans*, 45, 12144–12155
53. Pansare, A. V., Kulal, D. K., Shedge, A. A., & Patil, V. R. (2016). *J. Photoch. Photobio., B*, 162, 162473–162485
54. Pansare, A. V., Shedge, A. A., & Patil, V. R. (2018). *Int. J. Biol. Macromol*, 107, 1982–1987

55. Raja, D. S., Paramaguru, G., Bhuvanesh, N. S. P., Reibenspies, J. H., Renganathan, R., & Natarajan, K. (2011). *Dalton Trans*, 40, 4548–4559

56. Lu, X. L., Fan, J. J., Liu, Y., & Hou, X. A., J. Mol. Struct. 934(2009). 1–8.

57. Sen, T., Haldar, K. K., & Patra, A. J. (2008). *Phys. Chem. C*, 112, 17945–17951

58. Pansare, A. V., Shedge, A. A., Chhatre, S. Y., Das, D., Murkute, P., Pansare, S. V. … Chakrabarti, S. (2019). *J. Lumin*, 212, 133–140134

59. Ghosh, K., Rathi, S., & Arora, D. (2016). *J. Lumin*, 175, 135–140

Figures

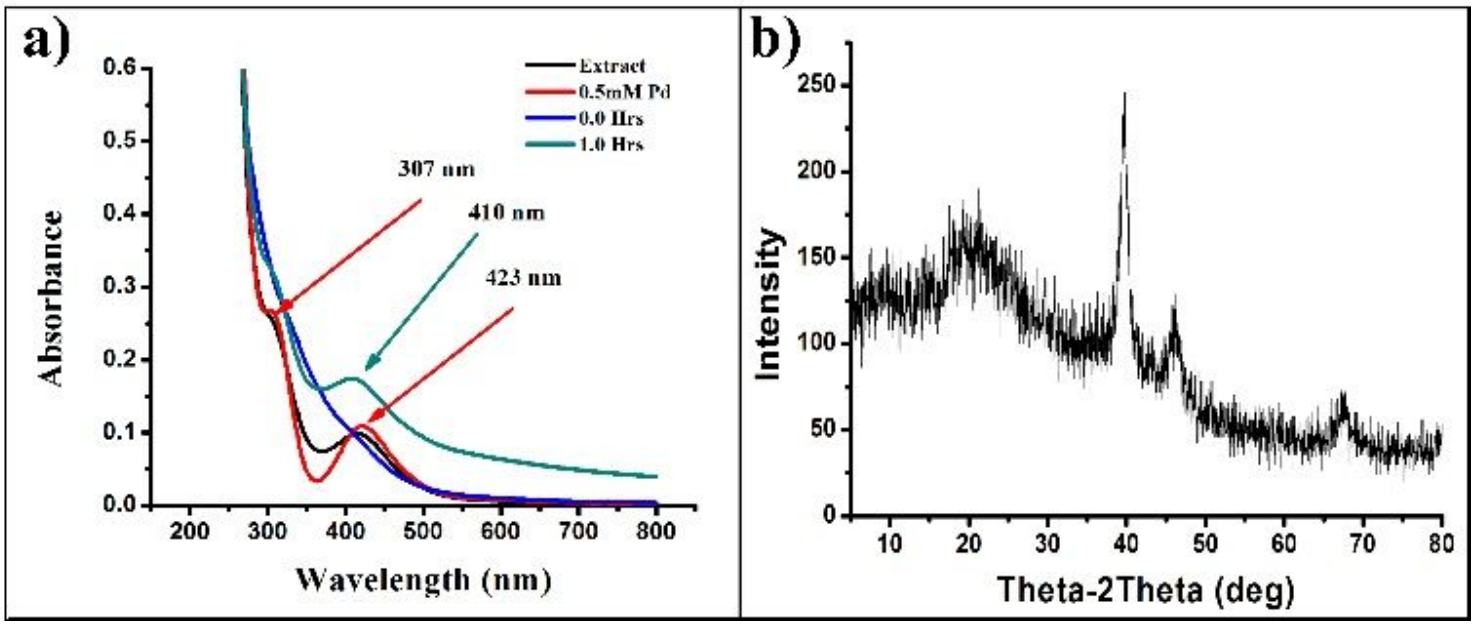

Figure 1

a) UV- Vis spectra recorded as a function of reaction time for the reaction of the 0.5mM PdCl2 solution with Aspergillus oryzae fungal stain. b) XRD diffraction pattern of PdNNs.

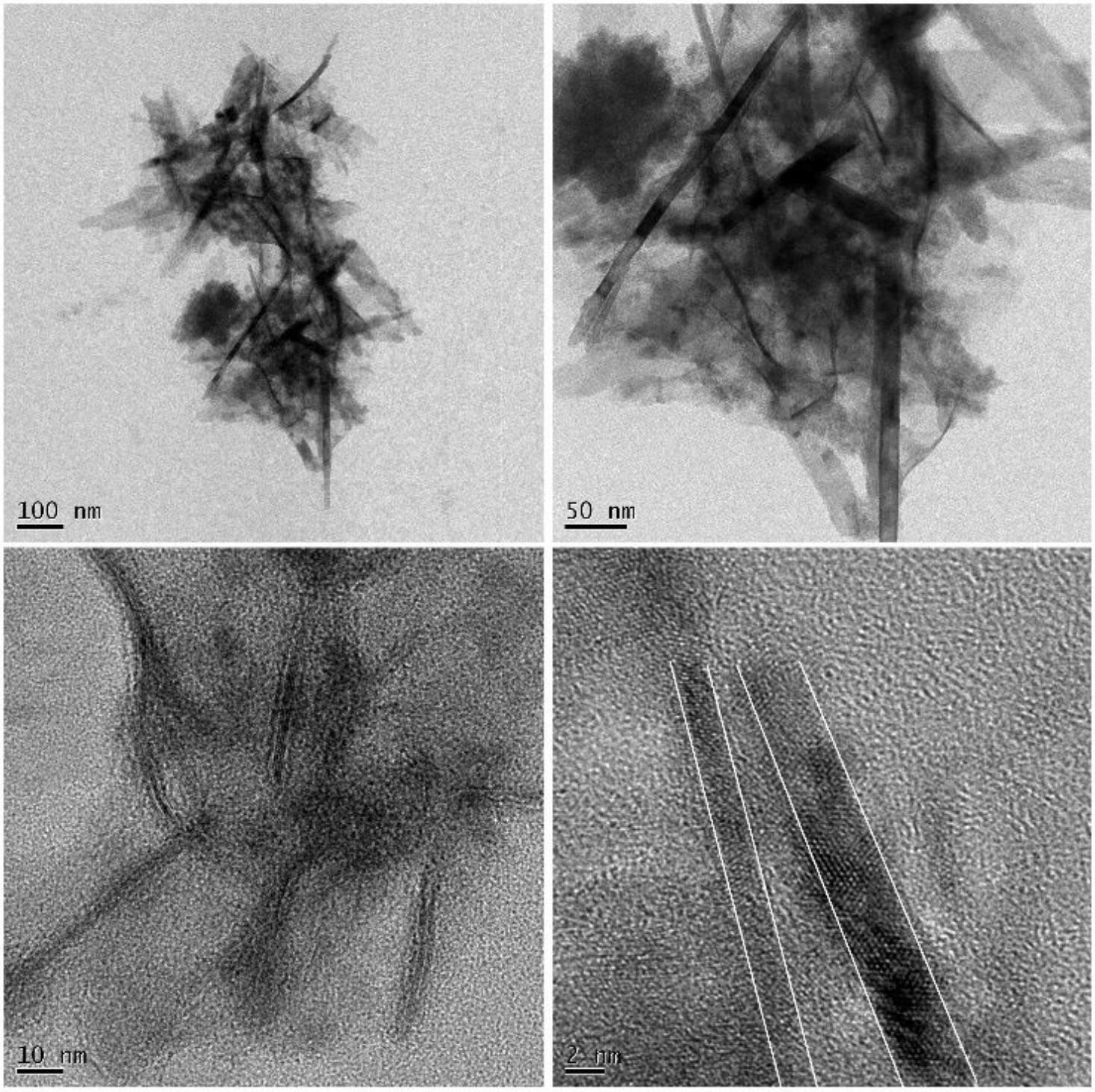

Figure 2

High resolution Transmission Electron Microscopy (HRTEM) of PdNNs.

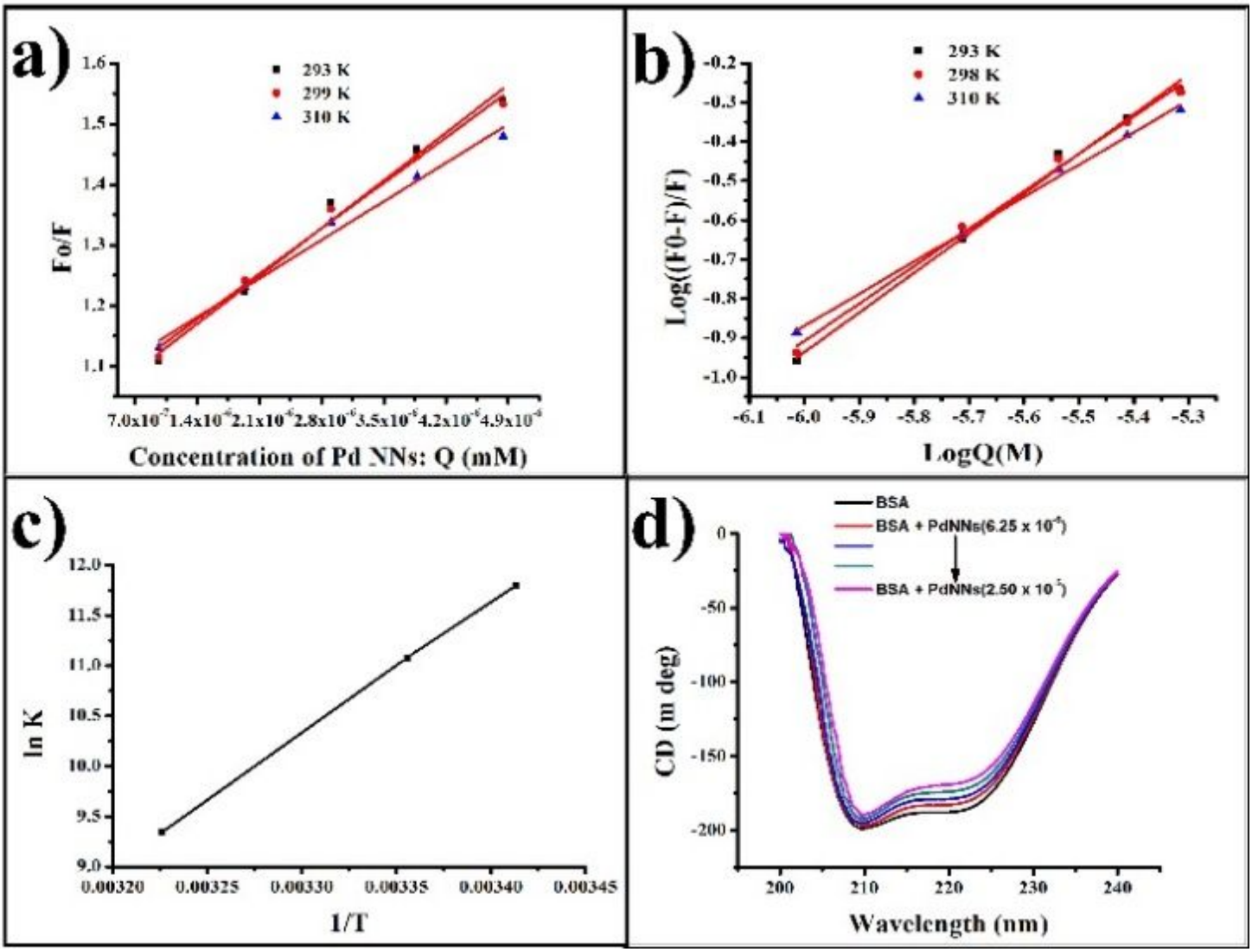

Figure 3

(a) Stern-Volmer plots for the quenching, (b) Double-logarithmic plot for the quenching of BSA by PdNNs and C) Plot of lnK vs. 1/T of the interaction between BSA and green synthesized PdNNs at 393 K,398 K, 310 K. d) CD spectra of BSA with PdNNs.

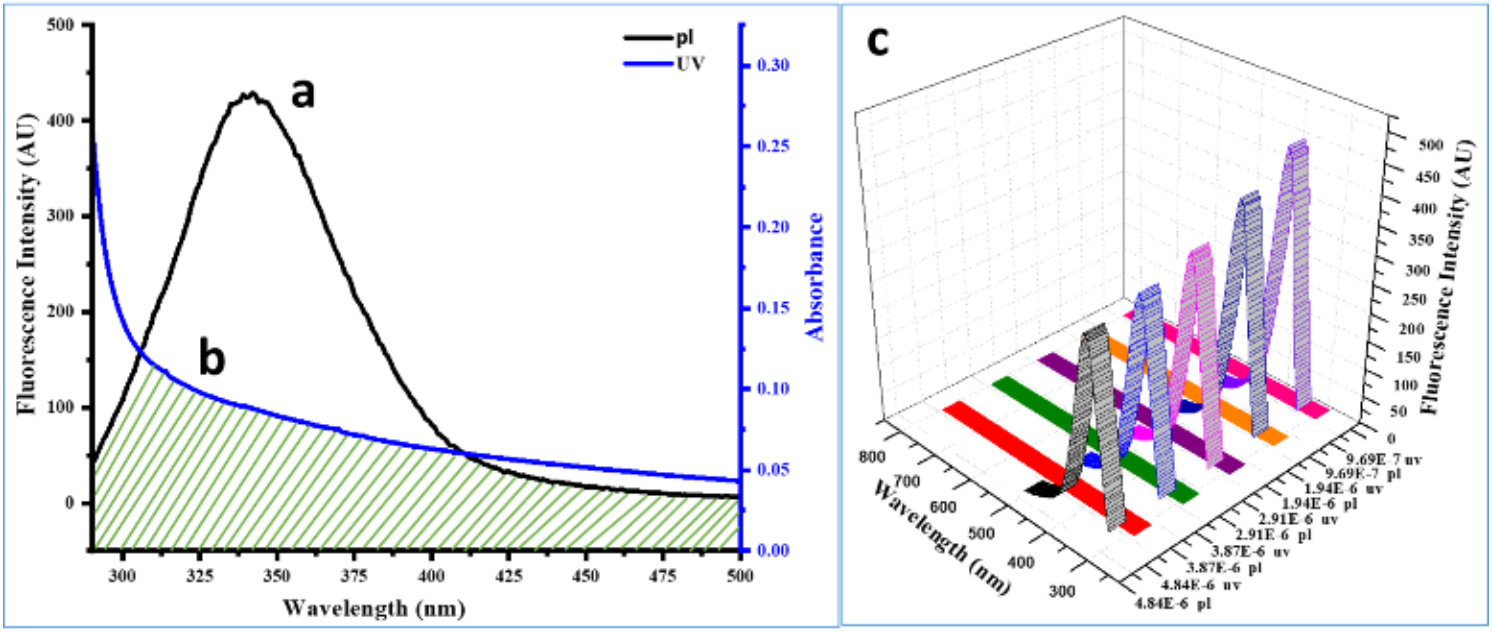

Figure 4

Overlap of the fluorescence spectra of BSA (T = 273 K) and the UV absorption spectrum of (a) Fluorescence spectrum of BSA (4.84 x 10−6 M); (b) UV absorption spectrum of PdNNs and BSA complex (4.84 x 10−6 M) c) overlap of the fluorescence spectra of BSA and the UV absorption spectrum (4.84 x 10−6 M to 9.69 x 10-7 M).

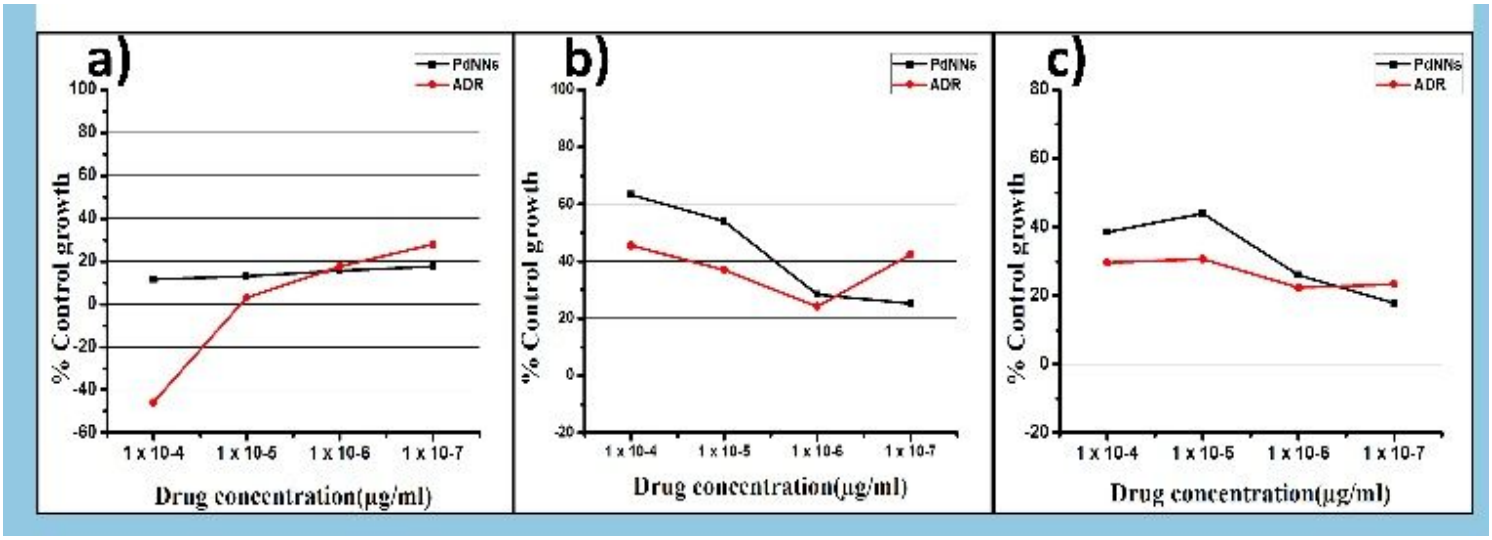

Figure 5

Percent control growth curve: Cancer Cell Line of green synthesized PdNNs and adriamycin a) MCF-7 b) COLO-205 c) K562.

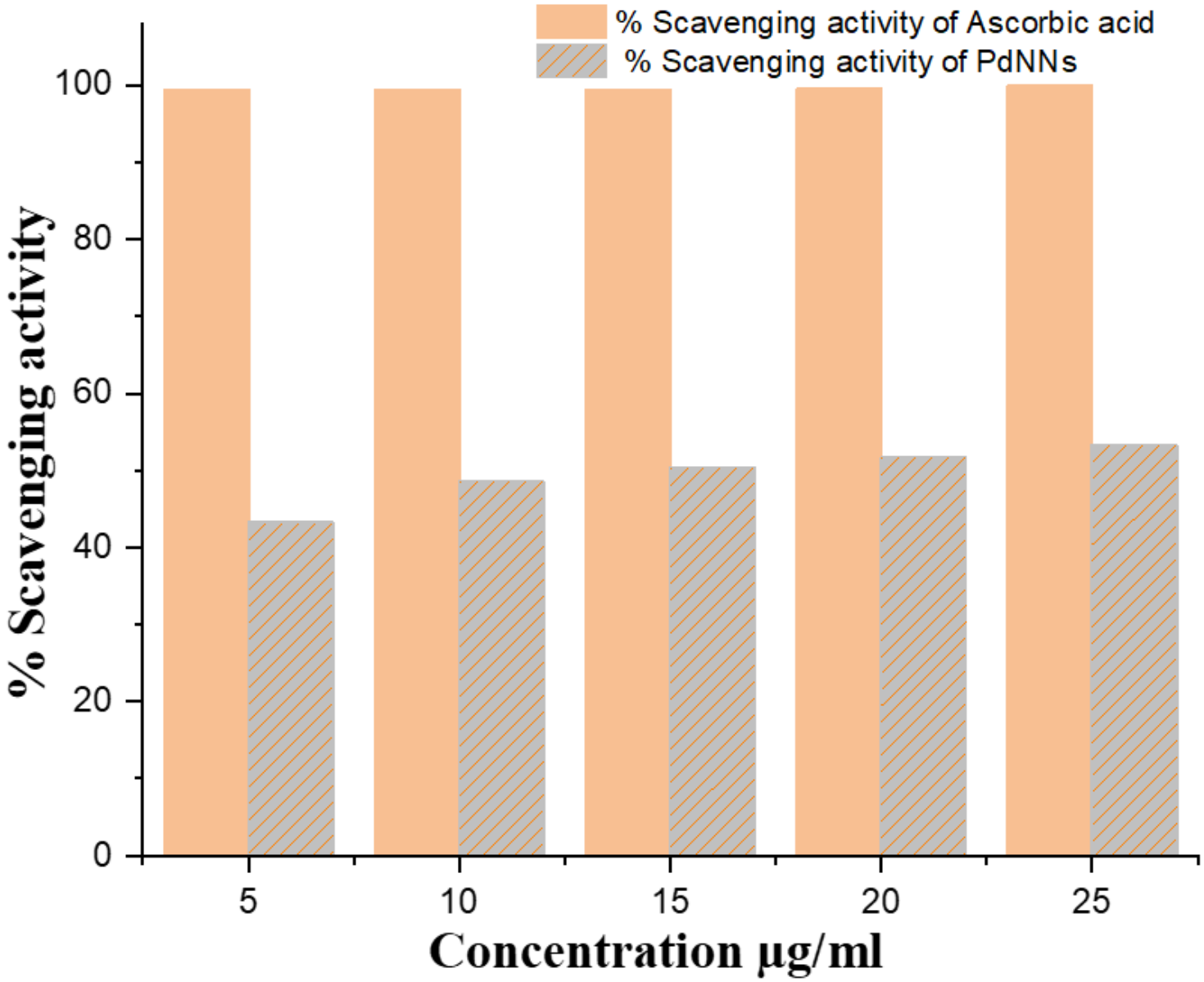

Figure 6

DPPH radical scavenging assay method for antioxidant activity of PdNNs compared with standard AA.

Supplementary Files

This is a list of supplementary files associated with this preprint. Click to download.

- SupportingInformation.docx